Solar Phys (2008) 247: 53–62
DOI 10.1007/s11207-007-9101-8

Microwave and Hard X-Ray Spectral Evolution for the 13 December 2006 Solar Flare

Zongjun Ning

Received: 17 June 2007 / Accepted: 28 November 2007 / Published online: 29 December 2007

Abstract This paper explores the time evolution of microwave and hard X-ray spectral indexes in the solar flare observed by Nobeyama Radio Polarimeters (NoRP) and the Ramaty High Energy Solar Spectroscopy Imager (RHESSI) on 13 December 2006. The microwave spectral index, γ_{MW}, is derived from the emissions at two frequencies, 17 and 35 GHz, and hard X-ray spectral index, γ_{HXR}, is derived from RHESSI spectra. Fifteen subpeaks are detected at the microwave and hard X-ray emissions. The microwave spectral indexes tend to be harder than hard X-ray spectral indexes during the flare, which is consistent with previous findings. All detected subpeaks follow the soft-hard-soft spectral behaviours in the hard X-ray rise-peak-decay phases. However, the corresponding microwave subpeaks display different spectral behaviour, such as soft-hard-soft, soft-hard-harder, soft-hard-soft + hard or irregular patterns. These contradictions reveal the complicated acceleration mechanism for low- and high-energy electrons during this event. It is also interesting that the microwave interpeak spectral indexes are much more consistent with one another.

Keywords Flares · Radio radiation · Hard X-rays

1. Introduction

The fact that microwave and hard X-ray emissions show similar profiles during a solar flare suggests that both are generated by a common population of energetic electrons. According to the standard model, when these electrons propagate along the lines of magnetic field toward the photosphere, they interact with the surrounding atmosphere and emit hard X-ray bremsstrahlung and gyrosynchrotron microwave radiation as they lose energy via Coulomb collisions in the lower atmosphere (*e.g.* Dennis and Schwartz, 1989). Observational evidence supports the idea that microwave and hard X-ray emissions are produced by nonthermal electrons in the lower solar atmospheric layer during flare eruption (*e.g.* Takakura and Kai, 1966; Kiplinger *et al.*, 1983; Nakajima *et al.*, 1983;

Z. Ning (✉)
Purple Mountain Observatory, Nanjing 210093, China
e-mail: ningzongjun@pmo.ac.cn

Gary, 1985; Schmahl, Kundu, and Dennis, 1985; Aschwanden, Benz, and Kane, 1990; Aschwanden, 1998; Bastian, Benz, and Gary, 1998; Asai *et al.*, 2001). A possible way to derive physical information from these nonthermal electrons is to study the spectral behaviours of microwave or hard X-ray emission. The spectral index can provide the most direct avenue for determining the distribution of nonthermal electrons and the energy they contain.

It was recognized early on that the hardness of the hard X-ray spectrum changes with time. There are three types of solar flares, characterized by their hard X-ray spectral behaviours as type A (thermal flares with a steep power law index greater than 7) (*e.g.* Tanaka, 1983; Ohki *et al.*, 1983; Tsuneta, 1985); type B (impulsive flares with a soft-hard-soft (SHS) spectral behaviour in the rise-peak-decay phases); and type C (gradual-hard flares following a soft-hard-harder (SHH) spectral pattern) (Parks and Winckler, 1969; Kane and Anderson, 1970; Frost and Dennis, 1971; Benz, 1977; Dennis, Frost, and Orwig, 1981; Brown and Loran, 1985; Dennis, 1985; Cliver *et al.*, 1986; Kiplinger, 1995; Fletcher and Hudson, 2002; Grigis and Benz, 2004). Previous observations show that the impulsive flares dominate or, at least, they are more frequent than gradual-hard events (*e.g.* Kosugi, Dennis, and Kai, 1988). Based on Nobeyama Radio Polarimeters (NoRP; Nakajima *et al.*, 1985) observations during cycle 23, Ning and Ding (2007) statistically studied the microwave spectral evolution in 103 solar flares, and found that the gradual-hard events (91 out of their samples) dominate in the microwave emission. This is consistent with previous results from data obtained by the Burst and Transient Source Experiment (BATSE) and the Owens Valley Radio Observatory (OVRO) (Marsh *et al.*, 1981; Alissandrakis, 1986; Nitta *et al.*, 1991; White and Kundu, 1992; Kundu *et al.*, 1994; Silva *et al.*, 1997; Silva, Wang, and Gary, 1999; Raulin *et al.*, 1999; Melnikov and Silva, 1999, 2000). Melnikov and Silva (1999, 2000) found that some solar flares decrease the microwave spectral index but simultaneously increase the hard X-ray spectral index during the decay phase. Of course, there are some examples of the gradual-hard events displaying their spectral evolution with a similar pattern on both microwave and hard X-ray emissions (*e.g.* Ning, 2007).

In this paper, we study the microwave and hard X-ray spectral behaviours for the 13 December 2006 flare, which shows multipeaks on both wavelengths. It is interesting that this event displays different spectral behaviours for the various subpeaks in microwave and hard X-ray emissions.

2. Observations

On 13 December 2006, a Geostationary Operational Environmental Satellite (GOES) satellite observed a soft X-ray event which started at 02:14 UT, with the maximum at 02:40 UT; the event ended at 02:57 UT. This event is classified as X3.4 and was located in the active region NOAA AR 0930 with a position S06W21. A high-speed Coronal Mass Ejection (CME) associated with this flare was observed by the Large Angle and Spectrometric Coronagraph (LASCO) instrument aboard the Solar and Heliospheric Observatory (SOHO). This flare was well observed by NoRP, RHESSI (Lin *et al.*, 2002), *Hinode* (Kosugi *et al.*, 2007) and other ground- or space-based instruments. The *Hinode* chromospheric (Ca II filter) observations show a well-known double-ribbon flare. This flare occurred just at the center of RHESSI's rotation. For technical reasons this means that hard X-ray imaging is very difficult. So we have lost a chance to make a detailed comparison of high-resolution flare images. However, the time profiles can be well studied from RHESSI data.

The microwave data that we use here was observed by NoRP, which works at seven discrete frequency channels at 1, 2, 3.75, 9.4, 17, 35 and 80 GHz with a time resolution of 0.1 s.

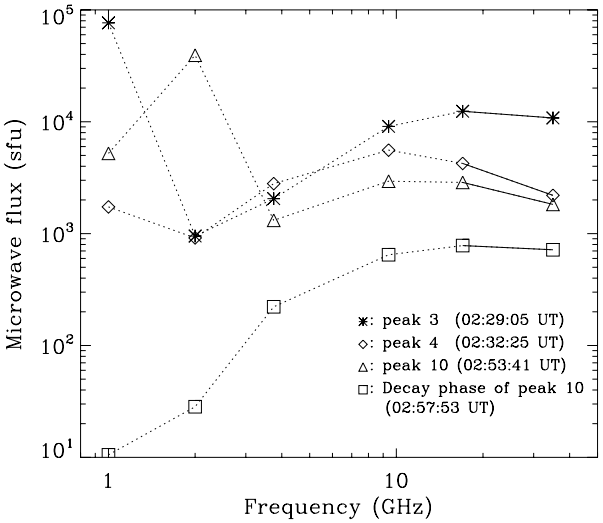

Figure 1 Microwave spectral plots at four discrete time intervals observed by NoRP on 13 December 2006. The frequencies of 17 and 35 GHz (dotted) are used to do spectral fitting (see text for details).

The microwave spectral index of nonthermal electrons, $\gamma(t)$, is derived from the flux spectral index, $\delta(t)$, as $\gamma(t) = -1.1[\delta(t) - 1.2]$ (*e.g.* Yokoyama *et al.*, 2002). The index of $\delta(t)$ can be computed when we assume a flux frequency dependence of the form $S(\nu, t) = F_0 \nu^{\delta(t)}$ (where $S(\nu, t)$ is the microwave radio flux (sfu) and ν is the frequency) in the optically thin part (*e.g.* Castelli and Guidice, 1976; Melnikov and Magun, 1998). We derive the microwave spectral index using only two channels, 17 and 35 GHz. The last channel of 80 GHz is excluded from spectral fitting due to the noise. Figure 1 shows the microwave spectra at four discrete times for this flare. In order to increase the signal-to-noise ratio, it is better to integrate the flux with respect to time (20 s in this paper) before doing microwave spectral fitting. The same method was used to statistically study the microwave spectral evolution from solar flares in the recent paper by Ning and Ding (2007).

The hard X-ray spectral index is derived from data observed by the RHESSI spacecraft, which observes over a broad wavelength range from hard X-rays to γ-rays. Its key features of high spectral resolution (1 keV in the X-ray range) and coverage of the low-energy range (down to 3 keV) allow us to separate the spectrum's thermal continuum from its nonthermal component, to study power law spectral evolution from the onset of the flare. We use the forward fitting method implemented by the Object Spectral Executive (OSPEX) code to derive the index of hard X-ray spectrum. The procedure requires us to use a photon spectra model featuring a power law with a low energy turnover in addition to a thermal emission. However, we have to first generate RHESSI count spectra in the uninterrupted sunlight time interval with a time binning equal to 20 s, and an energy binning of 2 keV from 3 to 300 keV. We use only the front segments of the detectors, and exclude the detectors 2 and 7. The same method to derive the hard X-ray spectral indexes was used by Ning (2007). We do spectral fitting above 10 keV to rule out the attenuator effects (*e.g.* Holman, 2005). Figure 2 shows the RHESSI spectral fitting results at four time intervals for the 13 December 2006, flare. The background emission has to be subtracted from an average before the start of the flare. The spectral shape is well represented by a broken power law plus a thermal component; see Figure 2(c). We limit the energy range to between 10 and 200 keV to do spectral fitting. There is no nonsolar particle background detected between 02:30 – 03:25 UT, while low levels are detected between 03:25 – 03:30 UT. The spectra are corrected for albedo from isotropically emitted hard X-ray photons. The pileup is weak after subpeak 4.

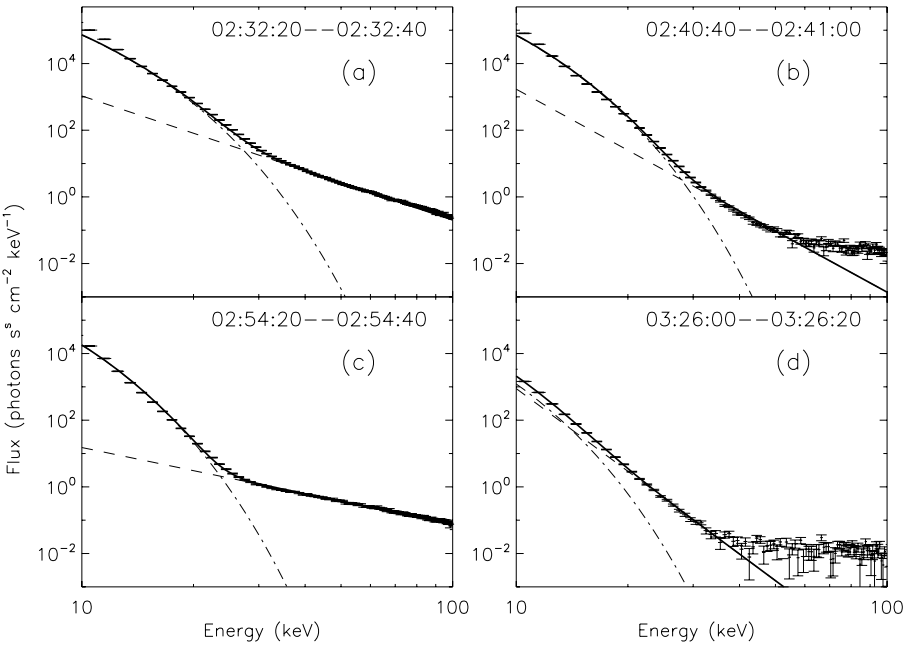

Figure 2 RHESSI spectra at four discrete time intervals for the 13 December 2006 flare. Dots with error bars represent the observational spectral data. Different lines show model spectral fits for thermal component (dot-dashed lines), nonthermal power law component (dashed-lines), and a summation of the two (thick-solid-lines).

3. Results

Figure 3 gives the time evolution of soft X-ray, hard X-ray and microwave emissions, and their spectral indexes for the 13 December 2006 flare observed by RHESSI between 02:30 UT and 03:30 UT. Fifteen subpeaks were observed by NoRP during this event, and 12 of them were also observed by RHESSI. Figure 3 shows that these 12 subpeaks display a soft-hard-soft spectral behaviour in the hard X-ray rise-peak-decay phases, which is consistent with the previous study from RHESSI data (Grigis and Benz, 2004). However, the microwave spectra show complicated behaviour.

3.1. Soft-Hard-Soft Pattern

The microwave subpeaks 1, 2 and 3 are missing from RHESSI observations. They follow soft-hard-soft (SHS) spectral behaviours in the microwave rise-peak-decay phases at 35 GHz. Anticorrelation between $\gamma_{\rm MW}$ and $F_{35\ \rm GHz}$ can be clearly seen. Figure 4 presents a logarithmic plot of $\gamma_{\rm MW}$ versus $F_{35\ \rm GHz}$ for subpeak 3 at the time interval between 02:27:20 UT and 02:31:20 UT. The plot with arrows clearly shows the overall SHS trend. Here arrows represent an average of three points. The cross-correlation coefficient of $\ln\gamma_{\rm MW}$ and $\ln F_{35\ \rm GHz}$ is -0.96, which indicates an anticorrelation behaviour between the spectral index and microwave flux. Although the spectral index does not vary clearly with the time, subpeak 5 tends to follow the SHS pattern.

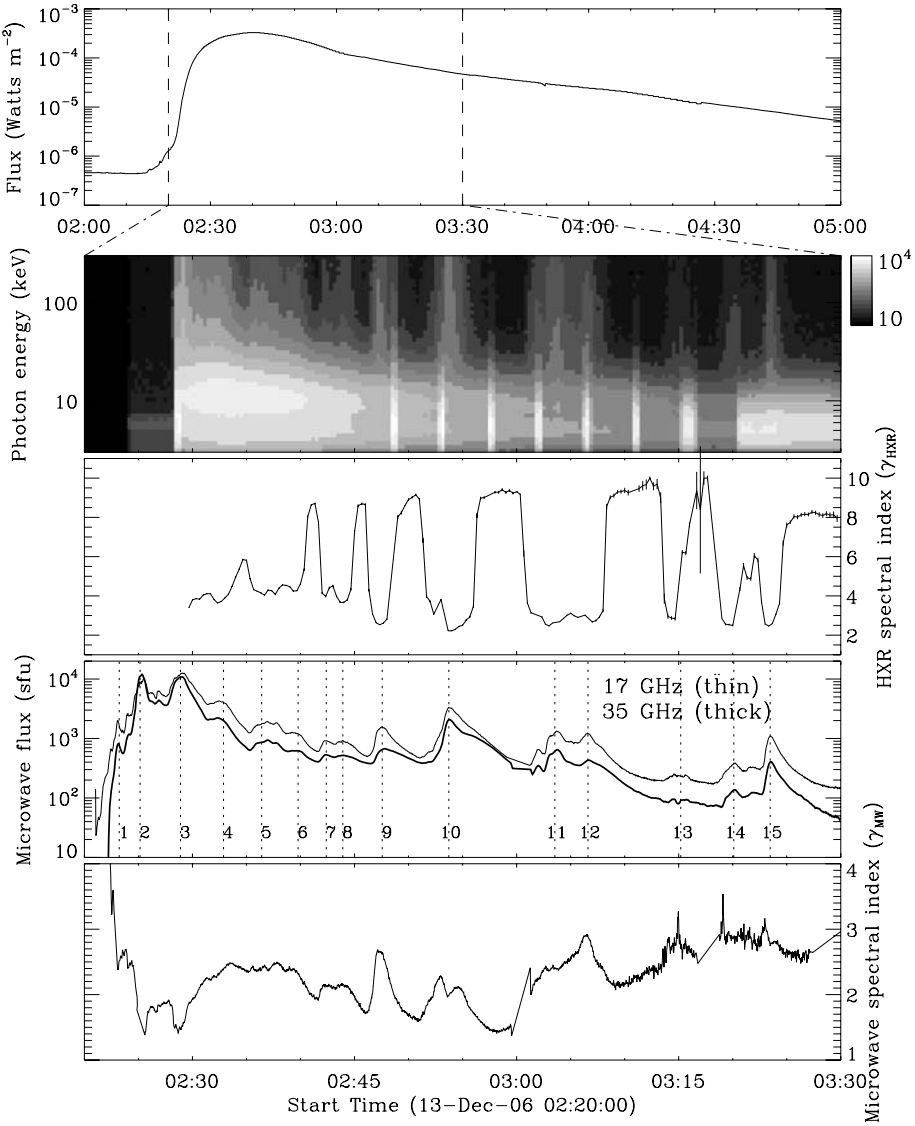

Figure 3 Time evolution of GOES soft X-ray, RHESSI hard X-ray, microwave emissions and their detected spectral indexes for the 13 December 2006 flare. Error bars for the hard X-ray spectral index are shown. The 15 subpeaks are marked with dotted lines and numbers.

3.2. SHH Pattern

The microwave subpeaks 6, 7, 8, 9 and 12 display the soft-hard-harder behaviours in their rise-peak-decay phases at 35 GHz. The microwave indexes rapidly soften in the rise phase, and reach the softest point before the maximum, then gradually harden with time from the peak to decay phases. In order to see clearly the microwave spectral behaviour, Figure 5 plots the time evolution of microwave and hard X-ray flux and spectral indexes for subpeak 9 in

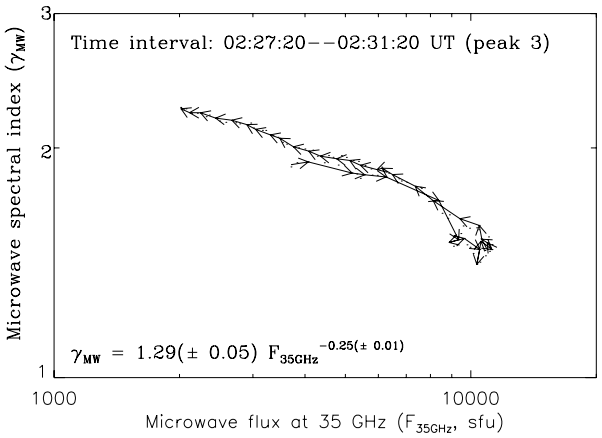

Figure 4 Plots of γ_{MW} versus the microwave flux at 35 GHz ($F_{35\ GHz}$) for subpeak 3. The arrows indicate the temporal evolution from the start to the end of this subpeak.

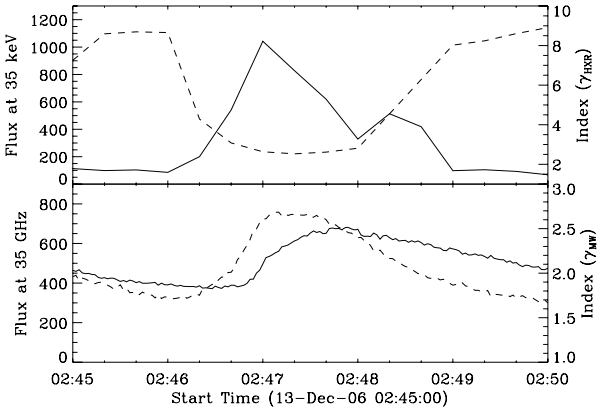

Figure 5 Microwave and hard X-ray emissions (solid) and their spectral index evolution (dashed) for subpeak 9.

detail. This subpeak is well observed at the microwave and hard X-ray emission. The hard X-ray presents a SHS pattern, while the microwave should show a SHH pattern. This result is consistent with previous findings for some individual flares (*e.g.*, White and Kundu, 1992; Kundu *et al.*, 1994; Silva *et al.*, 1997; Silva, Wang, and Gary, 2000; Raulin *et al.*, 1999; Melnikov and Silva, 1999, 2000). However, it seems that the microwave emission shows a hard-soft-hard pattern over the timescale of soft-hard-soft hard X-rays. The microwave subpeak 9 is observed tens of seconds later than that in hard X-rays. The harder spectral index before this microwave subpeak 9 should be due to the contribution from the decay phase of subpeak 8.

3.3. SHS + H Pattern

In these 15 microwave subpeaks, we find that some peaks have a complicated spectral evolution pattern, which shows a SHS pattern in the rise-peak-(preceding) decay phases, then continuously hardening on the following part of decay phase. That follows a soft-hard-soft + hard spectral pattern in the microwave rise-peak-decay phases. Thus, the microwave spectral index does not display similar behaviour during the decay phase. Subpeaks 10 and

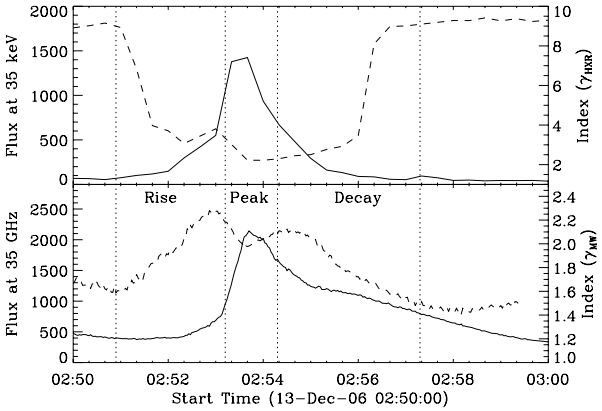

Figure 6 Microwave and hard X-ray emissions for subpeak 10. The rise-peak-decay phases are approximated by the dotted lines.

Table 1 Microwave and hard X-ray spectral patterns of 15 subpeaks for the 13 December 2006 flare.

Subpeak	1, 2, 3	4, 11	5, 13, 14	6, 7, 8, 9, 12	10, 15
γ_{MW}	SHS	Spe.	SHS	SHH	SHS+H
γ_{HXR}	–	SHS	SHS	SHS	SHS

15 belong to this type. It is the first time that such spectral behaviour has been detected in a solar flare. Similar to Figure 5, Figure 6 shows the time behaviours of subpeak 10 in detail. The rise-peak-decay phases are approximated and outlined for the microwave flux at 35 GHz. The spectral index of γ_{MW} is rapidly softening in the rise phase, hardens around the peak, and softens at the beginning of the decay phase; it then hardens again on the end of the decay phase. Figure 5 shows that the microwave index of about 0.2 from hard to soft around the maximum of the subpeak is reasonable. The error on the spectral index, which is detected using only two points each time, is zero.

3.4. Special Pattern

Subpeaks 4 and 11 show a special spectral pattern in the microwave emission. They do not belong to one of the preceding three types. The microwave spectral indexes of both subpeaks display an irregular pattern in the rise-peak-decay phases at 35 GHz.

Table 1 gives the microwave and hard X-ray spectral behaviours of 15 subpeaks for the 13 December 2006 flare.

4. Discussion and Conclusions

It is generally thought that nonthermal electrons at energies of many hundreds of keV radiate at microwave and at many tens of keV produce hard X-ray emissions in solar flares (*e.g.*, Melnikov and Magun, 1998; White *et al.* 2003). Information about these nonthermal electrons accelerated in solar flares can be deduced from the spectral features using the microwave and hard X-ray emissions. In this paper, we study the spectral evolution of the microwave and hard X-ray emissions for the 13 December 2006 solar flare observed by

NoRP and RHESSI. The event shows multiple peaks at both wavelengths. The microwave spectral index is harder than the hard X-ray index during this event, which is consistent with previous findings (*e.g.* White and Kundu, 1992; Kundu *et al.*, 1994; Silva *et al.*, 1997; Raulin *et al.*, 1999; Melnikov and Silva, 1999, 2000). All the subpeaks follow the soft-hard-soft spectral behaviour in the hard X-ray rise-peak-decay phases. However, the microwave subpeaks display four types of spectral patterns, such as SHS, SHH, SHS + H or irregular patterns. These contradictions indicate the different distribution of low- and high-energy electrons during this flare evolution.

4.1. Fitting Method Effects on Microwave Spectral Index

As noted earlier, the microwave spectral index is detected using only two channels, 17 and 35 GHz. It is not possible to use the 80 GHz channel to do spectral fitting. Although we increase the signal-to-noise at this channel by integrating a longer time interval, the high level of noise makes the flux at 80 GHz greater than that at 35 GHz (except for several subpeaks during 13 December 2006 flare). On the other hand, it is not certain that the emission at 17 GHz is purely optically thin during this event, especially at the time of subpeak 3 and the decay phase of subpeak 10 (see Figure 3). In other words, it is possible that there is an optically thick component, which heavily affects the spectral fitting. Such effects on the microwave spectral index cannot to be ruled out from the NoRP observations.

4.2. Acceleration or Emission Effects on Microwave Spectral Index

Subpeaks 6, 7, 8, 9 and 12 display that the microwave spectral flattening on the decay phase is accompanied by simultaneous spectral softening of the corresponding hard X-ray emission. These properties were interpreted as natural consequences of the nonstationary "trap + precipitation" model, which takes into account the energy spectrum hardening of trapped electrons due to Coulomb collisions as well as the difference between the spectral evolutions of injected and trapped electrons. The Coulomb collisions cause a shorter lifetime for lower energy electrons trapped in a magnetic loop. On the other hand, Lee and Gary (2000) showed that the evolution of nonthermal electrons' pitch-angle in a flaring loop can play an important role in the interpretation of the microwave spectral flattening. Another possibility is that the thermal emission contributes to the microwave emission at higher frequencies on the decay phase (*e.g.*, Ning and Ding, 2007), which is more reasonable for the subpeaks with complicated spectral patterns. If there is no thermal emission in the decay phase, these subpeaks could follow the soft-hard-soft spectral pattern at microwave as well as at hard X-ray. The thermal emission usually increases at the later phase, when the gyrosynchrotron emission is decreasing, especially at higher frequencies.

In this flare, the microwave subpeaks 4 and 11 show irregular spectral patterns, which could be because of overlap between subpeaks 3 and 4, or between subpeaks 10 and 11 at the microwave emission. This overlap could occur at one or both frequencies of 17 and 35 GHz. It is possible that the nonthermal electrons would be mixed in the flaring loops with the remaining electrons which were accelerated earlier.

It is an interesting fact that the interpeak spectral indexes are much more consistent with one another – *e.g.*, between peak 5 and peak 6, the microwave spectral index is around 2, similarly between peaks 7 and 8 and from before peak 11 to after peak 12. These kinds of differences are worth considering as well as their implications for the acceleration and microwave emission mechanisms.

Acknowledgements We thank the anonymous referee for his/her valuable comments to improve our manuscript. This work is supported by grants Y0607221222, 10333030, 10603014, 973 program (2006CB806302) and CAS project (KJCX2-YW-T04).

References

Alissandrakis, C.E.: 1986, *Solar Phys.* **104**, 207.
Asai, A., Shimojo, M., Isobe, H., Morimoto, T., Yokoyama, T., Shibasaki, K., Nakajima, H.: 2001, *Astrophys. J.* **562**, L103.
Aschwanden, M.J.: 1998, *Astrophys. J.* **502**, 455.
Aschwanden, M.J., Benz, A.O., Kane, S.R.: 1990, *Astron. Astrophys.* **229**, 206.
Bastian, T.S., Benz, A.O., Gary, D.E.: 1998, *Annu. Rev. Astron. Astrophys.* **36**, 131.
Benz, A.O.: 1977, *Astrophys. J.* **211**, 270.
Brown, J.C., Loran, J.M.: 1985, *Mon. Not. Roy. Astron. Soc.* **212**, 245.
Castelli, J.P., Guidice, D.A.: 1976, *Vistas Astron.* **19**, 355.
Cliver, E.W., Dennis, B.R., Kiplinger, A., Kane, S., Neidig, D.F.: 1986, *Adv. Space Res.* **6**, 249.
Dennis, B.R.: 1985, *Solar Phys.* **100**, 465.
Dennis, B.R., Schwartz, R.A.: 1989, *Solar Phys.* **121**, 75.
Dennis, B.R., Frost, K.J., Orwig, L.E.: 1981, *Astrophys. J.* **244**, L167.
Fletcher, L., Hudson, H.S.: 2002, *Solar Phys.* **210**, 307.
Frost, K.J., Dennis, B.R.: 1971, *Astrophys. J.* **165**, 655.
Gary, D.E.: 1985, *Astrophys. J.* **297**, 799.
Grigis, P.C., Benz, A.O.: 2004, *Astron. Astrophys.* **426**, 1093.
Holman, G.D.: 2005, *Adv. Space Res.* **35**, 1669.
Kane, S.R., Anderson, K.A.: 1970, *Astrophys. J.* **162**, 1003.
Kiplinger, A.L.: 1995, *Astrophys. J.* **453**, 973.
Kiplinger, A.L., Dennis, B.R., Frost, K.J., Orwig, L.E.: 1983, *Astrophys. J.* **273**, 783.
Kosugi, T., Dennis, B.R., Kai, K.: 1988, *Astrophys. J.* **324**, 1118.
Kosugi, T., Matsuzaki, K., Sakao, T., Shimizu, T., Sone, Y., Tachikawa, S., Hashimoto, T., Minesugi, K., Ohnishi, A., Yamada, T., Tsuneta, S., Hara, H., Ichimoto, K., Suematsu, Y., Shimojo, M., Watanabe, T., Shimada, S., Davis, J.M., Hill, L.D., Owens, J.K., Title, A.M., Culhane, J.L., Harra, L.K., Doschek, G.A., Golub, L.: 2007, *Solar Phys.* **243**, 3.
Kundu, M.R., White, S.M., Gopalswamy, N., Lim, J.: 1994, *Astrophys. J. Suppl. Ser.* **90**, 599.
Lee, J., Gary, D.E.: 2000, *Astrophys. J.* **543**, 457.
Lin, R.P., Dennis, B.R., Hurford, G.J., Smith, D.M., Zehnder, A., Harvey, P.R., Curtis, D.W., Pankow, D., Turin, P., Bester, M., Csillaghy, A., Lewis, M., Madden, N., van Beek, H.F., Appleby, M., Raudorf, T., McTiernan, J., Ramaty, R., Schmahl, E., Schwartz, R., Krucker, S., Abiad, R., Quinn, T., Berg, P., Hashii, M., Sterling, R., Jackson, R., Pratt, R., Campbell, R.D., Malone, D., Landis, D., Barrington-Leigh, C.P., Slassi-Sennou, S., Cork, C., Clark, D., Amato, D., Orwig, L., Boyle, R., Banks, I.S., Shirey, K., Tolbert, A.K., Zarro, D., Snow, F., Thomsen, K., Henneck, R., McHedlishvili, A., Ming, P., Fivian, M., Jordan, J., Wanner, R., Crubb, J., Preble, J., Matranga, M., Benz, A., Hudson, H., Canfield, R.C., Holman, G.D., Crannell, C., Kosugi, T., Emslie, A.G., Vilmer, N., Brown, J.C., Johns-Krull, C., Aschwanden, M., Metcalf, T., Conway, A.: 2002, *Solar Phys.* **210**, 3.
Marsh, K.A., Zirin, H., Hoyng, P., Dennis, B.R.: 1981, *Bull. Am. Astron. Soc.* **13**, 889.
Melnikov, V.F., Magun, A.: 1998, *Solar Phys.* **178**, 153.
Melnikov, V.F., Silva, A.V.R.: 1999, *ESA Spec. Publ.* **448**, 1053.
Melnikov, V.F., Silva, A.V.R.: 2000, In: Ramaty, R., Mandzhavidze, N. (eds.) *High Energy Solar Physics Workshop – Anticipating RHESSI. ASP Conf. Ser.* **206**, 371.
Nakajima, H., Kosugi, T., Kai, K., Enome, S.: 1983, *Nature* **305**, 292.
Nakajima, H., Sekiguchi, H., Sawa, M., Kai, K., Kawashima, S.: 1985, *Publ. Astron. Soc. Japan* **37**, 163.
Ning, Z.: 2007, *Astrophys. J.* **659**, L69.
Ning, Z., Ding, M.D.: 2007, *Publ. Astron. Soc. Japan* **59**, 373.
Nitta, N., White, S.M., Schmahl, E.J., Kundu, M.R.: 1991, *Solar Phys.* **132**, 125.
Ohki, K., Takakura, T., Tsuneta, S., Nitta, N.: 1983, *Solar Phys.* **86**, 301.
Parks, G.K., Winckler, J.R.: 1969, *Astrophys. J.* **155**, L117.
Raulin, J.-P., White, S.M., Kundu, M.R., Silva, A.V.R., Shibasaki, K.: 1999, *Astrophys. J.* **522**, 547.
Schmahl, E.J., Kundu, M.R., Dennis, B.R.: 1985, *Astrophys. J.* **299**, 1017.
Silva, A.V.R., Gary, D.E., White, S.M., Lin, R.P., de Pater, I.: 1997, *Solar Phys.* **175**, 157.

Silva, A.V.R., Wang, H., Gary, D.E.: 1999, In: Bastian, T.S., Gopalswamy, N., Shibasaki, K. (eds.) *Proceedings of the Nobeyama Symposium, Kiyosato, Japan, 27–30 October 1998*. NRO Report No. 479, **255**, 255.
Silva, A.V.R., Wang, H., Gary, D.E.: 2000, *Astrophys. J.* **545**, 1116.
Takakura, T., Kai, K.: 1966, *Publ. Astron. Soc. Japan* **18**, 57.
Tanaka, K.: 1983, *Astrophys. Space Sci. Lib.* **102**, 307.
Tsuneta, S.: 1985, *Astrophys. J.* **290**, 353.
White, S.M., Kundu, M.R.: 1992, *Solar Phys.* **141**, 347.
White, S.M., Krucker, S., Shibasaki, K., Yokoyama, T., Shimojo, M., Kundu, M.R.: 2003, *Astrophys. J.* **595**, L111.
Yokoyama, T., Nakajima, H., Shibasaki, K., Melnikov, V.F., Stepanov, A.V.: 2002, *Astrophys. J.* **576**, L87.